J. Fluid Mech. (1968), *vol.* 31, *part* 1, *pp.* 65–94
Printed in Great Britain

A transformation for compressible turbulent boundary layers with air injection

By L. O. F. JEROMIN
Engineering Department, University of Cambridge†

(Received 28 January 1967)

The transformation proposed by Coles for correlating the compressible turbulent boundary layer on a solid surface with a given incompressible layer has been extended to the case of a porous surface with air injection. However, unlike Coles's work, the new transformation does not use the empirical concept of the sublayer to define one of the transformation parameters. Instead this parameter can be defined in terms of the stream function at the wall, and so is directly related to the injection rate. The present paper concerns the transformation for the boundary layer with constant pressure and zero heat transfer, but the possibility of extending the transformation to flows with pressure gradients and heat transfer is mentioned briefly.

Comparison with experiments shows that the new transformation successfully relates c_f, θ and the fully turbulent part of the velocity profile with their corresponding incompressible values for a wide range of Mach numbers and injection rates.

1. Introduction

When fluid is injected through a porous wall into a turbulent boundary layer there are large changes in the characteristic of the layer. In particular the velocity profile is deformed in such a way that the skin friction and heat transfer coefficients are reduced. Further the actual flow of the injected fluid through the porous wall is a powerful method of cooling the wall. Thus fluid injection has wide engineering applications for cooling bodies exposed to high temperature gas streams, including the case of aircraft flying at high supersonic speeds. In this latter case the theoretical treatment of the problem involves the solution of the compressible turbulent boundary layer with injection of fluid (which may be different from the main stream fluid) at the wall. This is a formidable undertaking. However, there have recently been considerable developments in the corresponding incompressible problem (see, for example, Black & Sarnecki 1958; Stevenson 1963; McQuaid 1966). The purpose of the present paper is to extend the transformation techniques between compressible and incompressible boundary layers to the case of injection, and hence to make use of the incompressible knowledge.

A number of authors have proposed relatively simple transformation concepts for turbulent boundary layers assuming that the stream functions for the compressible flow and for the incompressible flow are the same. But these trans-

† Now at Messer Griesheim GmbH, Frankfurt/Main, Germany.

formations are too restrictive for the present purpose. A notable advance in the transformation technique was made by Coles (1962) who assumed that the stream functions in the two corresponding flows were not equal. This work was further extended to flows with pressure gradients and heat transfer and rationalized by Crocco (1963). Obviously the fact that the stream functions are not equal in the two flows increases the mathematical complexity of the transformation, but reduces the number of arbitrary assumptions. Thus the transformation of Coles and Crocco is practically free of any restrictions on the physical model. It is true that the substructure hypothesis does represent a compromise with the unknown nature of turbulence, but this hypothesis may be readily adapted as the theory of turbulence is developed. Recently Baronti & Libby (1966) investigated the correctness of a point-to-point mapping of compressible turbulent boundary-layer flow into its corresponding incompressible flow using Coles's transformation. They did not use Coles's substructure hypothesis but preferred to employ the assumption that the Reynolds number associated with the laminar sublayer is invariant. Baronti & Libby succeeded in correlating the compressible boundary-layer profile (up to a Mach number of $M = 6$) with the 'law of the wall' for the region where it normally holds for incompressible flow. Discrepancies arose, however, when they attempted to transform the outside part of the compressible boundary-layer profile into the 'velocity defect law'. They attributed these discrepancies to favourable pressure gradients, but it is possible that the reasons for the failure of the transformation in connexion with the velocity defect law are deeper and might be related to the sublayer concept itself.

Rosenbaum (1966) tried to extend Coles's transformation concept to compressible boundary layers with heat transfer and mass diffusion. He assumed that the incompressible flow field is completely known when the boundary layer is divided in the usual manner into a laminar sublayer, a region where the 'law of the wall' holds and another where the 'velocity defect law' is valid. The corresponding compressible flow field can easily be determined from the incompressible one with the help of Coles's transformation which is strictly valid in the form used there for zero heat transfer. However, contrary to Crocco,† Rosenbaum used the now-known compressible flow field to solve numerically the equations of conservation of energy and species assuming that the compressible boundary layer with heat transfer and mass diffusion can be reduced completely to a corresponding incompressible flow with zero heat transfer and zero mass diffusion. This has not been proved. Despite his questionable assumptions Rosenbaum obtained reasonable agreement between experimental data and his theoretical values for some boundary-layer characteristics.

1.1. *Present investigation*

The topic of the present paper is the extension of Coles's boundary-layer transformation to compressible turbulent boundary layers with air injection at the wall. The present paper concentrates on the case of zero pressure gradient and

† Crocco introduced transformation rules for the enthalpy distribution as well in order to transform the energy equation.

zero heat transfer. The transformation has been extended by the author to flows with heat transfer and pressure gradients (for details see Jeromin 1966*a*) The validity of the transformation has been checked in §3 for the simplest case of zero pressure gradient and zero heat transfer by transforming measured compressible boundary layers into their corresponding incompressible form making use of Stevenson's 'law of the wall'. In this way the skin friction coefficient has been evaluated with reasonable accuracy.

2. A boundary-layer transformation for the turbulent boundary layer with air injection

2.1. *The tranformation equations*

The starting point for the present investigation was Coles's transformation concept. He introduced the three transformation parameter σ, η and ξ which are defined in terms of the stream function ψ as follows:

$$\sigma(x) = \frac{\psi^*(x^*, y^*)}{\psi(x, y)}, \tag{2.1}$$

where

$$\left.\begin{aligned} \rho u &= \frac{\partial \psi}{\partial y}, \quad \rho^* u^* = \frac{\partial \psi^*}{\partial y^*}, \\ \rho v &= -\frac{\partial \psi}{\partial x}, \quad \rho^* v^* = -\frac{\partial \psi^*}{\partial x^*}, \end{aligned}\right\} \tag{2.2}$$

and

$$\eta(x) = \frac{\rho^*}{\rho}\frac{\partial y^*}{\partial y}, \tag{2.3}$$

$$\xi(x) = \frac{dx^*}{dx} \tag{2.4}$$

(the superscript * denotes incompressible flow), where u is the velocity in x-direction, v the velocity in y-direction and ρ the density. Coles showed that the three functions σ, η and ξ were functions of x only, or rather, that σ, x^* and $\partial y^*/\rho\,\partial y$ are independent of y if second-order derivatives are neglected.

The present analysis deals with boundary layers along a flat plate. The equations describing the compressible turbulent boundary layer along a flat plate are used in the present form:

continuity equation

$$\frac{\partial \rho u}{\partial x} + \frac{\partial \rho v}{\partial y} = 0; \tag{2.5}$$

momentum equation

$$\rho u \frac{\partial u}{\partial x} + \rho v \frac{\partial u}{\partial y} = -\frac{dp}{dx} + \frac{\partial \tau}{\partial y}; \tag{2.6}$$

with

$$\tau = \mu \frac{\partial u}{\partial y} - \rho \overline{u'v'},$$

where p is the pressure, τ the shear stress and μ the viscosity.

Every value in the equations (2.5) and (2.6) is regarded as a mean value unless otherwise specified.

The idea of the transformation is now to establish a correspondence with the simpler form of incompressible flow which has been more thoroughly investigated experimentallly as well as analysed theoretically. Corresponding to the relationships (2.5) and (2.6) the incompressible flow is described by the following equations:

continuity equation
$$\frac{\partial u^*}{\partial x^*}+\frac{\partial v^*}{\partial y^*}=0, \tag{2.5*}$$

momentum equation
$$\rho^* u^*\frac{\partial u^*}{\partial x^*}+\rho^* v^*\frac{\partial u^*}{\partial y^*}=-\frac{dp^*}{dx^*}+\frac{\partial \tau^*}{\partial y^*}; \tag{2.6*}$$

with
$$\tau^*=\mu^*\frac{\partial u^*}{\partial y^*}-\rho^*\overline{u^{*\prime}v^{*\prime}} \quad \text{and} \quad \rho^*=\text{constant}.$$

In order to apply the transformation one needs relationships which express the transformation parameters σ, η and ξ as functions of the boundary-layer characteristics. These relationships will not be derived here, since they are very similar to those already found by Coles (1962) and Crocco (1963). The only difference is the complicating condition of fluid injection at the wall which introduces additional terms. The main equations for the transformation parameters are

$$\frac{\sigma}{\eta}=\frac{u^*}{u}=\frac{u^*_\infty}{u_\infty} \tag{2.7}$$

and
$$\xi=\sigma\eta\frac{\rho_w\mu_w}{\rho^*\mu^*}\left\{1+\frac{2}{c_f}\left[\frac{d(\ln\sigma)}{dx}\left(\theta+\frac{\psi_w}{\rho_\infty u_\infty}\right)-\frac{1}{u_\infty}\frac{du_\infty}{dx}\int_0^\delta\left(1-\frac{\rho}{\rho_\infty}\right)dx\right.\right.$$
$$\left.\left.-\left[\delta^*+\theta-\int_0^\delta\left(1-\frac{\rho}{\rho_\infty}\right)dy\right]\frac{d(\ln\eta/\sigma)}{dx}\right]\right\}, \tag{2.8}$$

where the subscript ∞ refers to free-stream condition, and w to the wall condition. The boundary-layer thickness δ, the skin-friction coefficient c_f, the displacement thickness δ^* and the momentum thickness θ are defined in the usual way.

The equations (2.7) and (2.8) can be found by introducing (2.1) to (2.4) in (2.5) and (2.6), (2.5*) and (2.6*) respectively. It can be shown (see Jeromin 1966*a*) that a correspondence for the inertia and pressure gradient terms in (2.6) and (2.6*) can be established mathematically exactly. The weak point at the transformation is the deduction that the shear stress terms can be transformed as well, which cannot be proved in general because of the unknown shear stress distribution in physical as well as mathematical terms. Consequently one cannot be sure if the shear stress distribution of the compressible boundary layer can be reduced to the corresponding incompressible one and hence if

$$\tau^*=\frac{\sigma^2}{\xi\eta}\left[\tau+\frac{1}{\sigma}\frac{d\sigma}{dx}\int_0^y\psi\frac{\partial u}{\partial y}dy+\rho_\infty u_\infty\frac{\sigma}{\eta}\frac{d}{dx}\left(\frac{\eta}{\sigma}\right)\int_0^y\frac{\rho}{\rho_\infty}\left(\frac{u^2}{u_\infty^2}-1\right)dy+\frac{dp}{dx}\int_0^y\left(1-\frac{\rho}{\rho_\infty}\right)dy\right] \tag{2.9}$$

really holds.† The validity of (2.9) and hence the final proof for a general application of the transformation can only be checked by measuring shear stress profiles

† For the derivation of (2.8) see Coles (1962) or Jeromin (1966*a*).

in compressible flow and reducing them to those in corresponding incompressible flow.

It must be pointed out here that all the relations (2.1) to (2.9) are independent of any viscosity law and energy equation so that they can be applied to laminar and turbulent flow and to flow with and without mass transfer.

Up to this point the present analysis is very similar to those by Coles and Crocco. The conclusions now drawn from the equations (2.1)–(2.8), and the application of the transformation itself, run along a different path adapting the problem to the more special case of turbulent boundary layers with fluid injection.

2.2. *Evaluation of the transformation parameters for zero pressure gradient and zero heat transfer*

2.2.1. *Differential equation for the parameter* σ

Only two relationships have been given so far for the three transformation parameters σ, η and ξ, namely the equations (2.7) and (2.8). These equations reduce for the case of constant pressure to

$$\frac{\sigma}{\eta} = \frac{u^*}{u} = \frac{u_\infty^*}{u_\infty} = \text{constant} \tag{2.7}$$

with $u_\infty^* = \text{constant}$, $u_\infty = \text{constant}$ and to

$$\xi = \sigma\eta \frac{\rho_w \mu_w}{\rho^* \mu^*} \left\{ 1 + \frac{2}{c_f} \left(\theta + \frac{\psi_w}{\rho_\infty u_\infty} \right) \frac{1}{\sigma} \frac{d\sigma}{dx} \right\}. \tag{2.8'}$$

The physical interpretation of the relation $\sigma/\eta = \text{constant}$ is the condition that the compressible flow with zero pressure gradient transforms into an incompressible flow with the same physical feature of vanishing pressure gradients (for details of the choice $\sigma/\eta = \text{constant}$ see Coles 1962 and Crocco 1963). Equation (2.7) means simply that the velocity scale between the two flows can be chosen arbitrarily without influencing the transformation at all. Consequently it is not necessary to prescribe the physical properties of the incompressible flow except for u_∞^*, ρ^* and μ^* which can be chosen arbitrarily as long as the density is a function of the temperature alone. Moreover, Crocco pointed out that one obtains the same transformation if the incompressible fluid chosen is a liquid or a gas.

So far one has found two relationships for the three unknown parameters σ, η and ξ.

One now needs a third relationship to complete the transformation. This third relationship will probably vary from problem to problem and at the moment cannot be derived from the equations of motion. For example, Coles showed that

$$d\sigma/dx = 0$$

for laminar boundary layers and turbulent wakes, and he introduced a substructure hypothesis as a third relationship in order to apply the transformation to turbulent boundary layers.

Present transformation. Another approach to the problem, completely different from Coles's substructure concept, can be used for the case of fluid injection using

the definition equation (2.2). The stream functions ψ and ψ^* must hold all through the boundary layer and so at the wall. Thus

$$\psi_w^* = -\int_0^{x^*} \rho^* v_w^* \, dx^* \tag{2.10*}$$

and

$$\psi_w = -\int_0^{x} \rho_w v_w \, dx, \tag{2.10}$$

when the virtual origin of the flow is set to zero for both the incompressible and compressible flow which is no restriction to the problem. The transformation parameter can then be written as

$$\sigma = \frac{\psi_w^*}{\psi_w} = \frac{\rho^* v_w^* x^*}{\rho_w v_w x} \tag{2.11}$$

by assuming that $\rho^* v_w^*$ and $\rho_w v_w$ are constant along the wall. It should be noted here that the choice of $\rho^* v_w^* =$ constant and $\rho_w v_w =$ constant is quite arbitrary. The injection mass flow along the wall was set constant because this condition corresponds to the experimental investigation which will be analysed in § 3 with the help of the present boundary-layer transformation. In principle the transformation parameter σ can be defined more generally replacing the numerator in (2.11) by (2.10*) and the denominator by (2.10).

A disadvantage of the definition of the transformation parameter σ in terms of the stream function (2.10) and (2.10*) is the fact that flows without mass transfer are not contained in the present analysis as a limiting case. For zero injection (2.11) becomes indeterminate even when one tries to approach this limiting case by assuming very small injection rates $\rho_w v_w$ and $\rho^* v_w^*$. Consequently another relationship has to be used to obtain σ for $F^* = 0$ and $F = 0$ which might be for example Coles's substructure hypothesis ($F^* = v_w^*/u_\infty^*$, $F = \rho_w v_w/\rho_\infty \mu_\infty$).

Equation (2.11) is the third relationship defining, together with the equations (2.7) and (2.8′), all three transformation parameters.† It is postulated here that a compressible boundary layer with fluid injection transforms into an incompressible one with fluid injection at the wall. Moreover, it is assumed that an incompressible flow with a given injection mass flow $\rho^* v_w^*$ can be chosen arbitrarily within a certain range without affecting the transformation, as will be shown later when applying the law of corresponding stations (see § 2.2.2). From (2.11) it can be deduced that a transformation parameter σ is defined for any given compressible flow with an injection mass flow $\rho_w v_w$ and at a Reynolds number R_x (in other words the variable x is fixed, too) together with corresponding incompressible flows with any assumed injection mass flow $\rho^* v_w^*$. A given compressible flow with given $\rho_w v_w$ and x can be transformed into an incompressible flow with $\rho^* v_w^*$, but the location x^* in the transformed flow corresponding to the point x in the compressible flow changes with the injection mass flow $\rho^* v_w^*$ in order to fulfil equation (2.11); or once x^* is chosen the injection mass flow

† Equation (2.11) fulfils the condition that σ is only dependent on x, x^* respectively, since $\rho^* v_w^*$ and $\rho_w v_w$ are only functions of x^*, x respectively and independent of the coordinate y.

$\rho^* v_w^*$ is defined. Since it is the aim of a transformation to use established incompressible laws, only transformations for which both flows can be physically realized will be considered.

It will be here assumed that a given compressible flow at a certain Reynolds number R_x will transform into incompressible flows at fairly high Reynolds numbers, say in the order of 10^7 where this number is chosen quite arbitrarily. Now it was said that the compressible flow can be transformed into an incompressible flow with any injection rate. It is quite possible that a number of such flows are separated at this high Reynolds number,† most likely those with higher injection rates, so that the physical reality limits the concept and hence the number of possible incompressible flows. There might be still a pure mathematical transformation possible for the case of separation, but since it is the aim of a transformation to use only established incompressible laws, this prospect is only of academic interest.

Differentiating equation (2.11) with respect to x and making use of (2.4) gives

$$\frac{d\sigma}{dx} = \frac{\rho^* v_w^*}{\rho_w v_w}\left[\frac{1}{x}\frac{dx^*}{dx} - x^*\frac{1}{x^2}\right],$$

and from (2.11) it follows that

$$\xi\frac{d\sigma}{dx^*} = \frac{\sigma}{x^*}\xi - \frac{\rho_w v_w}{\rho^* v_w^*}\frac{\sigma^2}{x^*},$$

or alternatively

$$\xi = \frac{\rho_w v_w}{\rho^* v_w^*}\frac{\sigma}{x^*}\left[\frac{\sigma}{x^*} - \frac{d\sigma}{dx^*}\right]^{-1}. \tag{2.12}$$

Eliminating ξ from (2.12) and (2.8′), and assuming that $c_f^*(x^*)$, $\theta^*(x^*)$ and all properties of the incompressible flow are known, one finally obtains

$$\frac{d\sigma}{dx^*} = \frac{\sigma^2 - A\sigma}{\sigma x^* + 2A\dfrac{v_w^*}{u_\infty^* c_f^*}x^* - 2A\dfrac{\theta^*}{c_f^*}}, \tag{2.13}$$

where

$$A = \frac{u_\infty^*}{u_\infty}\frac{\rho^*\mu^*}{\rho_w\mu_w}\frac{\rho_w v_w}{\rho^* v_w^*}. \tag{2.14}$$

The integration of (2.13) gives the variation of the transformation parameter σ with x. A closed solution for (2.13) can be obtained for Dutton's (1958) flow with asymptotic suction where $c_f^* = -2v_w^*/u_\infty^*$, $v_w^* =$ constant and $\theta^* =$ constant. This possibility will be mentioned here only for reason of completeness, since the main task of the present analysis is a transformation for the compressible turbulent boundary layer with injection. In general, (2.13) cannot be solved analytically, but a numerical method can be used instead. If $\sigma(x)$ is known the other two parameters can easily be calculated using (2.7) and

$$\xi = \sigma\left(\sigma + \frac{2Av_w^*}{u_\infty^* c_f^*} - 2A\frac{\theta^*}{c_f^* x^*}\right)\left[\frac{u_\infty^*}{u_\infty}\frac{\rho^*\mu^*}{\rho_w\mu_w} + \frac{\rho^* v_w^*}{\rho^* u_\infty^*}\frac{u_\infty^*}{u_\infty}\frac{\rho^*\mu^*}{\rho_w\mu_w}\frac{2}{c_f^*} - \frac{2}{c_f^*}\frac{u_\infty^*}{u_\infty}\frac{\rho^*\mu^*}{\rho_w\mu_w}\frac{\theta^*}{x^*}\right]^{-1}. \tag{2.15}$$

Equation (2.15) is obtained by introducing (2.13) in (2.8′) and eliminating ξ.

† This statement will be discussed in more detail in § 2.2.2.

Finally, the transformations for the most important boundary-layer parameters will be specified since they will be used later:

skin friction coefficient
$$c_f^* = \frac{1}{\sigma}\frac{\rho^*\mu^*}{\rho_w\mu_w}\frac{\rho_\infty}{\rho^*}c_f; \tag{2.16}$$

momentum thickness
$$\theta^* = \eta\frac{\rho_\infty}{\rho^*}\theta; \tag{2.17}$$

displacement thickness
$$(\delta^*)^* = \eta\frac{\rho_\infty}{\rho^*}\left[\delta^* - \int_0^\delta\left(1-\frac{\rho}{\rho_\infty}\right)dy\right]; \tag{2.18}$$

skin friction
$$\tau_w^* = \frac{\sigma}{\eta^2}\frac{\rho^*\mu^*}{\rho_w\mu_w}\tau_w; \tag{2.19}$$

Reynolds number per unit length
$$R^* = \frac{\sigma}{\eta}\frac{\mu_\infty}{\mu^*}\frac{\rho^*}{\rho_\infty}R; \tag{2.20}$$

Reynolds number based on x
$$R_x^* = \frac{\sigma^2}{\eta}\frac{\mu_\infty}{\mu^*}\frac{\rho^*}{\rho_\infty}\frac{\rho_w v_w}{\rho^* v_w^*}R_x; \tag{2.21}$$

Reynolds number based on θ
$$R_\theta^* = \sigma\frac{\mu_\infty}{\mu^*}R_\theta; \tag{2.22}$$

longitudinal co-ordinate x
$$x^* = \frac{\rho_w v_w}{\rho^* v_w^*}\sigma x; \tag{2.23}$$

normal co-ordinate
$$y^* = \eta\int_0^y\frac{\rho}{\rho^*}dy; \tag{2.24}$$

injection mass flow normal to the wall at $y = y^* = 0$
$$\rho^* v_w^* = \frac{\sigma}{\xi}\frac{\sigma^2 x + \dfrac{2AF^*}{c_f^*} - \dfrac{u_\infty^*}{u_\infty}\dfrac{\rho^*\mu^*}{\rho_w\mu_w}\left(2\dfrac{\theta^*}{c_f^*} - \xi x\right)}{\dfrac{2AF^*}{c_f^*} + 2\dfrac{\theta^*}{c_f^*}\dfrac{u_\infty^*}{u_\infty}\dfrac{\rho^*\mu^*}{\rho_w\mu_w}}\rho_w v_w. \tag{2.25}$$

2.2.2. *Starting condition for the integration of equation* (2.13)

A starting condition must be known before (2.24) can be integrated. This relation is most likely an empirical one considering the incomplete knowledge of the turbulent mechanism. So far it has not been necessary to introduce an empirical relationship in order to define directly a transformation parameter. The empirical relations $c_f^* = f(R_x^*)$ and $\theta^* = f(R_x^*)$ cannot be regarded as relationships defining a transformation parameter itself but only as relationships which have to be known before the transformation can be applied. In that sense they are no empirical restriction to the definition of the transformation parameter as expressed by the equations (2.7), (2.8′) and (2.11).

A successful method for the evaluation of a starting condition was derived from the transformation of the skin friction coefficient (2.16) and the definition

equation for σ (2.11), which compares experimental data obtained in incompressible and compressible flow with fluid injection. By introducing (2.11) into (2.16) one obtains

$$c_f = \frac{\rho^* v_w^*}{\rho_w v_w}\frac{x^*}{x}\frac{\rho_w \mu_w}{\rho^* \mu^*}\frac{\rho^*}{\rho_\infty} c_f^* = \frac{\rho^* v_w^*}{\rho_w v_w}\frac{\rho_w \mu_w}{\rho^* \mu^*}\frac{\rho_\infty^*}{\rho_\infty}\frac{R_x^*}{R_x}\frac{\mu^*}{u_\infty^* \rho^*}\frac{u_\infty \rho_\infty}{\mu_\infty} c_f^*,$$

or

$$\frac{\rho_\infty \mu_\infty}{\rho_w \mu_w} c_f F R_x = c_f^* F^* R_x^*, \tag{2.26}$$

with

$$F = \rho_w v_w / \rho_\infty u_\infty \quad \text{and} \quad F^* = v_w^*/u_\infty^*.$$

Coles obtained a similar relationship for flow without injection

$$\frac{\rho_\infty \mu_\infty}{\rho_w \mu_w} c_f R_\theta = c_f^* R_\theta^*, \tag{2.27}$$

which he called the 'law of corresponding stations' so that (2.26) can be regarded as another form of the 'law of corresponding stations' for flows with fluid injection. It might be worth noting that (2.27) holds for flows with air injection as well. Equation (2.26) is more useful than (2.27) for the present process of evaluating a starting condition for the integration of (2.13) since it expresses the starting point in terms of x as necessary and not in terms of θ.

Equation (2.16) can be written as

$$\sigma = \frac{\rho_\infty}{\rho_w}\frac{c_f}{c_f^*}\frac{\mu^*}{\mu_w} = \frac{\rho_\infty}{\rho_w}\frac{\mu^*}{\mu_w}\frac{(c_f/F)}{(c_f^*/F^*)}\frac{F}{F^*} = \frac{\rho_\infty \mu^* \rho_w v_w \rho^*}{\rho_w \mu_w \rho^* v_w^* \rho_\infty}\frac{u_\infty^*}{u_\infty}\frac{(c_f/F)}{(c_f^*/F^*)}$$

or finally

$$\sigma = A(c_f/F)/(c_f^*/F^*). \tag{2.28}$$

The equations (2.26) and (2.28) together present an empirical method for evaluating a starting condition for the integration.

Equation (2.26) can be interpreted physically by saying that a correspondence between incompressible flow and compressible flow exists at positions where the product $(\rho_\infty \mu_\infty/\rho_w \mu_w)\, c_f F R_x$ of the compressible flow is equal to the product $c_f^* F^* R_x^*$ for the corresponding incompressible flow. Hence known boundary-layer characteristics like the skin-friction coefficient c_f or the momentum thickness θ can be used with the help of the equations (2.16) or (2.17) to determine the transformation parameters when the corresponding positions in both kinds of flows have been found for which a transformation exists. In the following this concept will be used to determine a starting condition for the integration of (2.13) by plotting c_f/F against $(\rho_\infty \mu_\infty/\rho_w \mu_w)\, c_f F R_x$, c_f^*/F^* against $c_f^* F^* R_x^*$ respectively, and comparing incompressible and compressible data at

$$c_f^* F^* R_x^* = \frac{\rho_\infty \mu_\infty}{\rho_w \mu_w} c_f F R_x = \text{constant}.$$

The parameter in such a diagram† is the injection rate F or F^*. Such a diagram is shown in figure 1. The incompressible data for the parameter F^* are represented

† These co-ordinates have been chosen according to (2.26). As ordinate could be chosen c_f or $c_f F$ instead of c_f/F without affecting the result for σ as defined by (2.28) (c_f/F is more convenient on mathematical grounds by considering (2.28)). The essential meaning of (2.26) is that one set of data (compressible) can be compared with another one (incompressible) at

$$\frac{\rho_\infty \mu_\infty}{\rho_w \mu_w} c_f F R_x = c_f^* F^* R_r^* = \text{constant}.$$

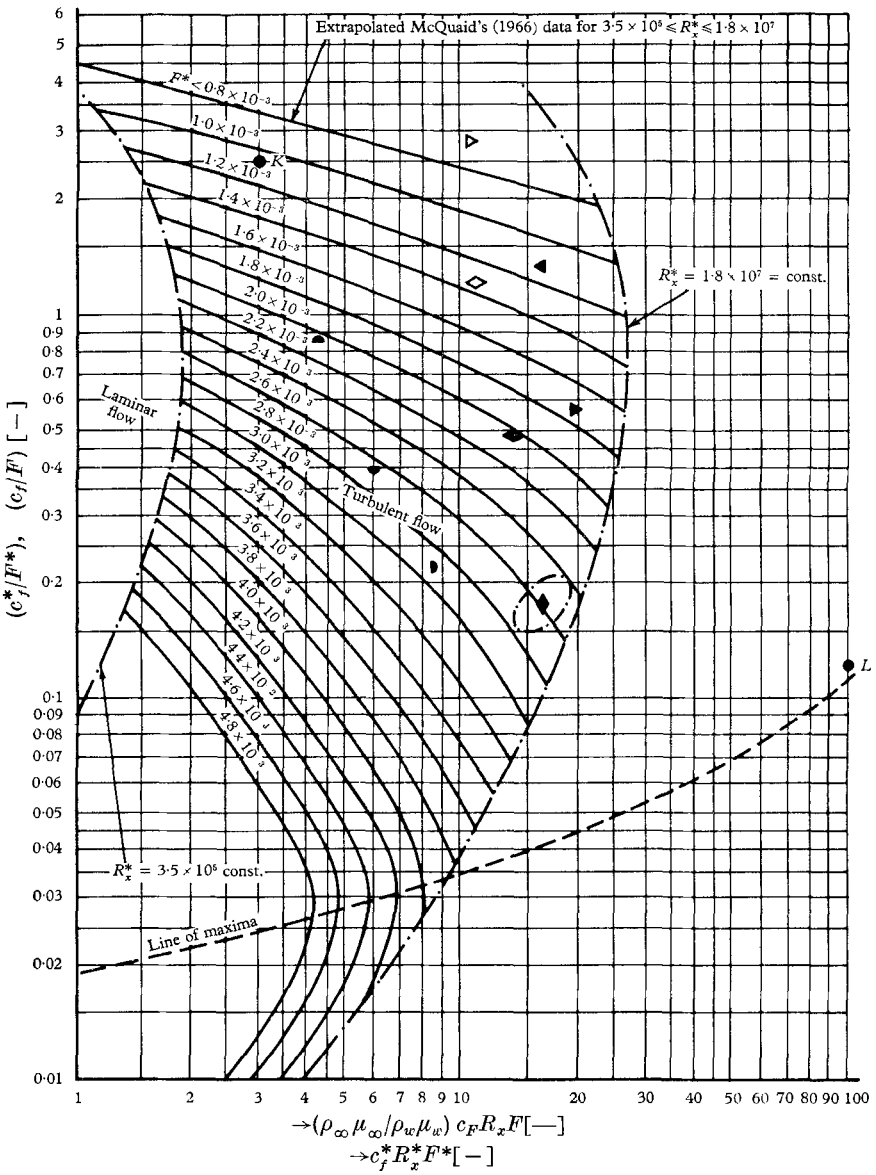

FIGURE 1. Correlation between compressible and incompressible flow obtained by 'law of corresponding stations'.

Symbol	$F\times10^3$ [−]	M [−]	Investigator
●	0·8756	6·2	Danberg (1964)
●	1·745	6·2	
●	2·444	6·2	
▷	0·570	2·5	Jeromin (1966*b*)
◀	0·895	2·5	
▶	1·271	2·5	
◇	0·653	3·5	
◆	1·172	3·5	
◆	2·111	3·5	

by the solid lines whereby the value of c_f/F decreases with increasing $c_f^* F^* R_x^*$ for $F^* =$ constant. The influence of the parameter F^* in figure 1 is such that an increase of F^* causes a shift of the curves towards the left-hand corner in the diagram. The solid lines are evaluated from McQuaid's (1966) experimental data (see appendix). The reason for this choice is the fact that these data have to be considered as the most reliable ones at present available as the investigation by McQuaid (1966) has shown. Unfortunately only a limited amount of experimental data is available for compressible turbulent boundary layers along flat plates with air injection and zero heat transfer. These are the investigations of Danberg (1964) at a Mach number of 6·2 and Jeromin (1966*b*) at a Mach number of 2·5 and 3·5. It must be noted that both sets of data are not measured at exactly adiabatic wall conditions. Danberg's wall temperature is slightly lower than the adiabatic wall temperature, whereas Jeromin's data are measured at wall temperatures slightly above adiabatic. But these effects can be considered as being probably insignificant in their influence on the skin-friction coefficient. Possible effects lie certainly within the range of uncertainty for c_f considering the fact that the skin-friction coefficients are subject to a possible error of the order of at least $\pm 10\,\%$ (for high injection rates the error could easily increase to $\pm 40\,\%$), since they are evaluated from the slope at the wall $\partial u/\partial y$ (Danberg 1964), or the momentum equation (Jeromin 1966*b*), respectively. The compressible data are marked by the symbols on figure 1. The Reynolds number influence on the compressible data has been neglected so that only mean Reynolds numbers are considered and hence only points appear in figure 1 instead of lines. The reasons for this approximation are:

(i) the Reynolds number range covered by the experimental investigations (Jeromin: $1{\cdot}6 \leqslant R_x \times 10^{-7} \leqslant 1{\cdot}8$) is quite small compared to the range covered in incompressible flow;

(ii) Danberg's published data for the skin-friction coefficient are subject to a scatter which has sometimes opposite tendencies to the Reynolds number influence.

Depending on the possible error for the skin-friction coefficient the symbols on figure 1 representing the compressible flow might shift. The error becomes quite large for the relatively high injection rate of $F = 2{\cdot}111 \times 10^{-3}$ at $M = 3{\cdot}5$ and is indicated by the dotted line around the corresponding symbol.

A few words must be said about figure 1 since it presents experimental evidence for possible transformations from compressible to incompressible flow. The region of turbulent flow which can be observed physically is limited on the left-hand side on figure 1 by a line, or better a region of transition to laminar flow and on the right-hand side by a maximum for every injection rate. Beginning from the maximum, $c_f^* F^* R_x^*$ decreases again for decreasing c_f^*/F^* until the point with $c_f^* = 0$ is reached which cannot be shown on figure 1 because of the logarithmic scale. The line of maxima in figure 1 must be regarded for the time being as a pure qualitative one which is not yet justified by any theory or experimental data at all and partly extrapolated for higher injection rates from McQuaid's data. The empirical relations defining the skin-friction coefficient in the presence of fluid injection as derived by Jeromin (1966*a*) from McQuaid's (1966) data are rather

doubtful for high injection rates and especially for high Reynolds numbers so that the lines for $F^* > 4{\cdot}8 \times 10^{-3}$ have to be discounted until more experimental information for this region is available. The existence of the maxima especially have to be proved more generally, since it would mean that a compressible flow

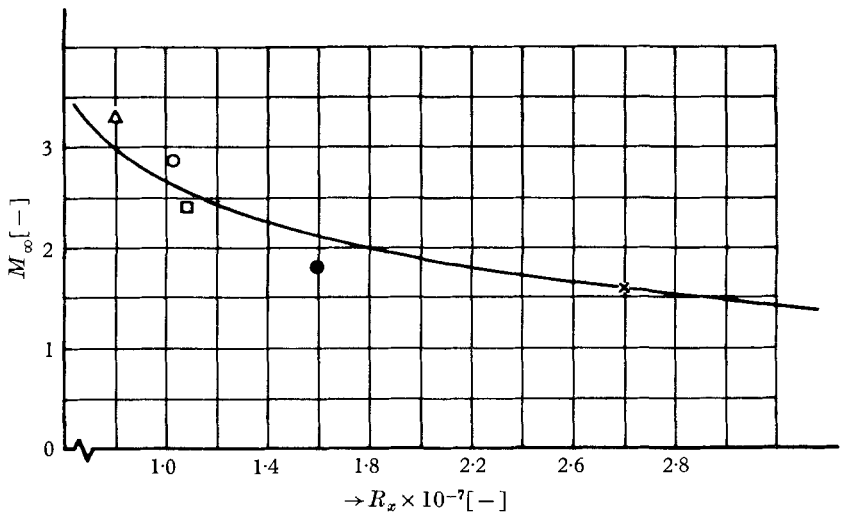

FIGURE 2. Effect of Mach number on transition point for flow along solid flat plate. ×, Czarnecki & Sinclair (1955); ●, Scherrer (1951); □, Higgins & Pappas (1951); ○, Eber (1952); △, Van Driest & Boison (1955).

at a Reynolds number R_x could be transformed into two corresponding Reynolds numbers in an incompressible flow at the same injection rate. For example, a point in a compressible flow characterized by $(\rho_\infty \mu_\infty / \rho_w \mu_w)\, c_f F R_x = 3$ can be transformed to two different points representing incompressible flows with an injection rate of $F^* = 4{\cdot}8 \times 10^{-3}$, namely with $c_f^*/F^* = 0{\cdot}057$ and $c_f^*/F^* = 0{\cdot}013$ and hence with two different Reynolds numbers R_x^*. The limiting lines in figure 1 are most probably influenced by compressibility and heat transfer effects. For example, the critical Reynolds number decreases with increasing Mach number and changing adiabatic wall condition as shown in figure 2 (see also Schlichting 1960) where the critical Reynolds number is plotted against the Mach number.

Transformations from one flow to another are possible within this range limited by the maxima and transition lines. An example might clarify the situation. A compressible flow characterized by the point K at

$$c_f^* F^* R_x^* = \frac{\rho_\infty \mu_\infty}{\rho_w \mu_w} F c_f R_x = 3$$

can be transformed to corresponding incompressible flows with at least all the injection rates F^* considered in figure 1. On the other hand a compressible flow at the point L in figure 1 at $c_f^* F^* R_x^* = (\rho_\infty \mu_\infty / \rho_w \mu_w) F c_f R_x = 100$ near the line of maxima can only be transformed into flows with injection rates $F^* < 1{\cdot}8 \times 10^{-3}$ since no flow with higher injection rates F^* exists in this range.

The transformation parameter σ was evaluated from figure 1 for

$$c_f^* F^* R_x^* = (\rho_\infty \mu_\infty / \rho_w \mu_w)\, c_f F R_x = 10$$

comparing the available compressible data with those for incompressible flow making use of (2.28), where A is mainly a function of the Mach number and the injection rates.† The compressible data were extrapolated to $c_f^* F^* R_x^* = 10$ assuming that they show the same tendency with $(\rho_\infty \mu_\infty / \rho_w \mu_w)\, c_f F R_x$ as the solid lines representing the incompressible flow with $c_f^* F^* R_x^*$. It was deduced from (2.11) that one can choose incompressible flows with injection rates F^* arbitrarily. Applying this concept to figure 1, one can read from the diagram a set of values c_f^*/F^* at $c_f^* F^* R_x^* = (\rho_\infty \mu_\infty / \rho_w \mu_w)\, c_f F R_x = 10$ for every compressible flow characterized by one value c_f/F. Hence the corresponding incompressible flows are characterized by the set of values c_f^*/F^* and cover, in the present case, a range of injection rates $0{\cdot}8 \leqslant F^* \times 10^3 \leqslant 3{\cdot}6$. The transformation parameter can be determined now from (2.43) knowing c_f/F, A and a set of values c_f^*/F^*. The result is plotted in figure 3 against F^*/F where the ordinate was given preference against any other because this plot seems to suppress all Mach number effects. (F increases steadily in the direction of the arrow in figure 3 independently from which set of data for compressible flow in figure 1 σ was evaluated.) It also gives $\sigma = f(F^*/F)$ for F = constant, which is a very convenient relationship to express the starting condition for the integration of (2.13) in an explicit form.

But it must be stressed here that there is still the possibility that this clear tendency expressed in figure 3 might be somehow fortuitous, since the value for σ is subject to the same error as the skin-friction coefficient itself. The error for σ can be considerable for $\sigma < 2{\cdot}5$ in the region of the steep gradient $d(F^*/F)/d\sigma$ so that especially for higher injection rates (F in the order of 2×10^{-3}) the curves might shift. To clarify the situation it might be worth giving an example. Choosing an injection rate for the incompressible flow of $F^* = 2 \times 10^{-3}$ results in possible errors of

$$\Delta\sigma = \pm 0{\cdot}15 \quad \text{for} \quad F = 0{\cdot}570 \times 10^{-3} \quad \text{at} \quad M = 2{\cdot}5,$$
$$\Delta\sigma = \pm 0{\cdot}5 \quad \text{for} \quad F = 2{\cdot}111 \times 10^{-3} \quad \text{at} \quad M = 3{\cdot}5.$$

The error $\Delta\sigma$ decreases when higher injection rates F^* for the corresponding incompressible flow are chosen. But, nevertheless, the correlation in figure 3 is surprisingly good when one neglects the possible errors for the skin-friction coefficient and uses only the published data. Data taken by two different investigators at three different Mach numbers for each of three injection rates have been correlated in figure 3 so that the well-defined tendencies (especially for the parameter F independent which Mach number was chosen) exhibited in this

† $c_f^* F^* R_x^* = 10$ was chosen because most of the experimental data for compressible transpired boundary layers are measured in the range $7 \leqslant (\rho_\infty \mu_\infty / \rho_w \mu_w)\, c_f F R_x \leqslant 20$. One could in principle compare incompressible and compressible data at other values $c_f^* F^* R_x^* =$ constant and so evaluate the transformation parameter by a sort of interpolation method for various Reynolds numbers instead of integrating (2.12). This concept has been checked for $c_f^* F^* R_x^* = 3$ by comparing the interpolated results for σ with those evaluated from (2.13) using the starting point $c_f^* F^* R_x^* = 10$. The results agreed within 10% for $F = 1{\cdot}271 \times 10^{-3}$ at $M = 2{\cdot}5$.

diagram can be partly employed for the justification of the postulate in §2.2.1 that a compressible flow can be transformed in a corresponding incompressible one with an injection rate chosen arbitrarily.

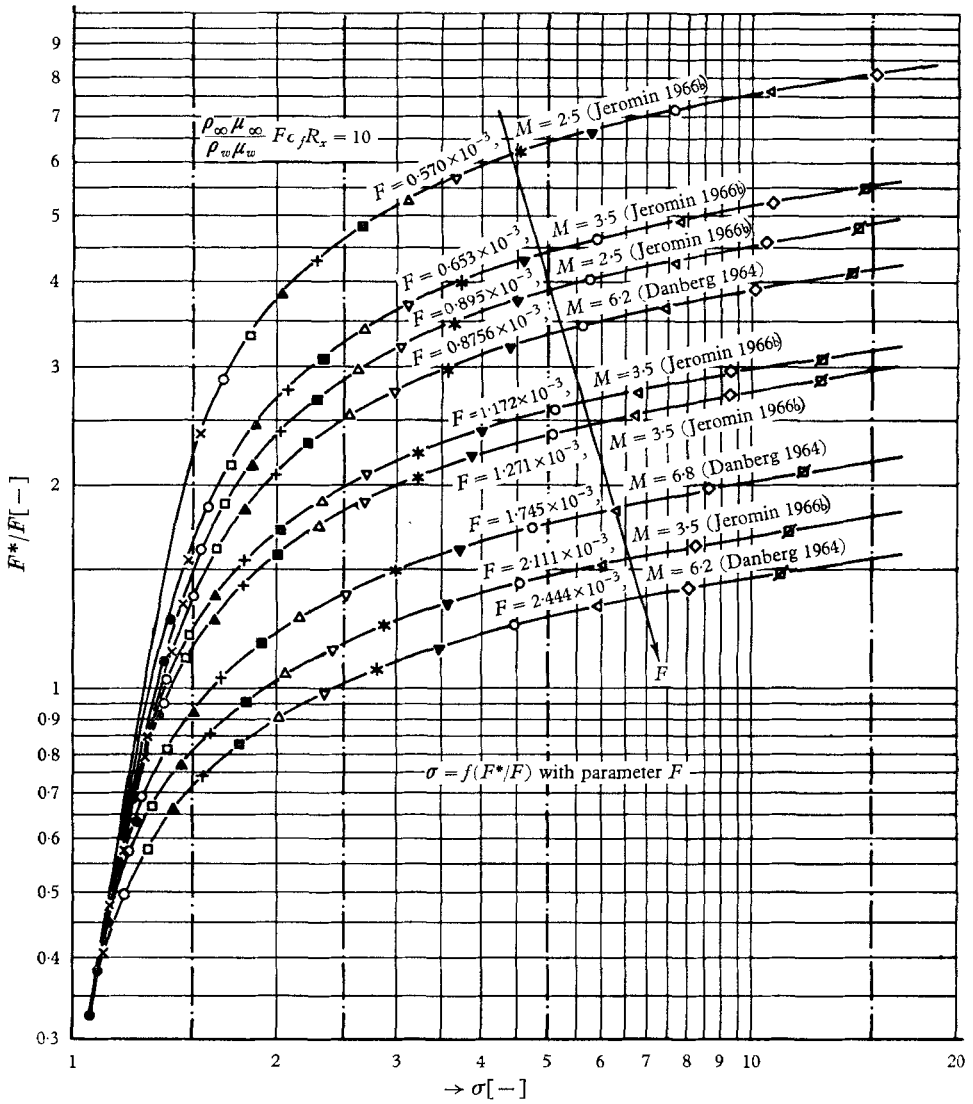

FIGURE 3. Empirical evaluation of a starting-point for the integration of (2.13) making use of the 'law of corresponding stations' and available experimental data. $F^* \times 10^3$ (McQuaid, 1966): ○, 0·8; ×, 1·0; ○, 1·2; □, 1·4; △, 1·6; +, 1·8, ■, 2·0; ▲, 2·2; ▽, 2·4; ∗, 2·6; ▼, 2·8; ○, 3·0; ▷, 3·2; ◇, 3·4; □, 3·6.

2.2.3. *The determination of the transformation parameters*

In performing the integration it is convenient to use dimensionless equations by multiplying (2.13) by $1/R^*$. Thus one obtains

$$\frac{d\sigma}{dR_x^*} = \frac{\sigma^2 - A\sigma}{\sigma R_x^* + 2AF^*(R_x^*/c_f^*) - 2A(R_\theta^*/c_f^*)}. \tag{2.13'}$$

These equations have been integrated on the Titan (Atlas II) Computer in the University Mathematical Laboratory, Cambridge, for both parameters F and F^*.

In every case, F is held constant and F^* is varied from its initial value of $0{\cdot}8 \times 10^{-3}$. The highest injection rate F^* for an incompressible flow considered

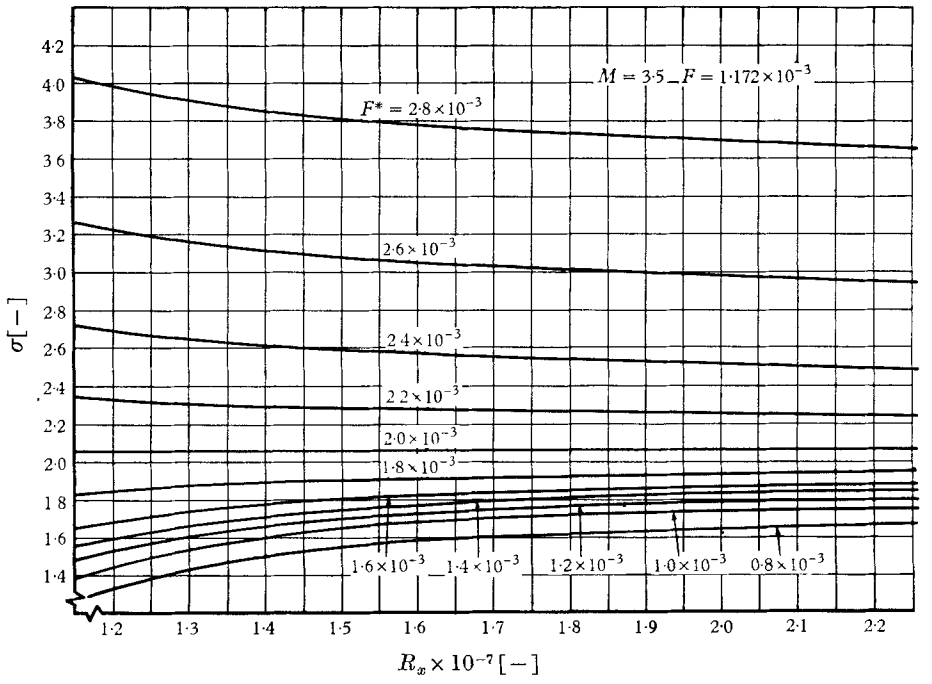

FIGURE 4. Variation of the transformation parameter σ with the Reynolds number R_x.

in this analysis was $F^* = 3 \times 10^{-3}$. The calculation results in a set of tables or graphs for every Mach number and injection rate F and only a typical case will be given here. The transformation parameter (calculated from (2.13′)) is plotted against the Reynolds number R_x on figure 4. Once σ is known the other transformation parameters η and ξ can be calculated from equations (2.7) and (2.8′). They are plotted on figures 5 and 6. These three graphs represent the key to the transformation, which in this particular case is for compressible flow along an adiabatic wall at a Mach number of 3·54 and an injection rate of $F = 1{\cdot}172 \times 10^{-3}$ into a corresponding incompressible flow with injection rates of $0{\cdot}8 \leqslant F^* \times 10^3 \leqslant 3$, a free-stream velocity of $u_\infty^* = 16{\cdot}0$ [m/s], a temperature $t^* = 20$ [°C] and a pressure of $\rho^* = 1$ [atm]. The quantities for the incompressible flow may be chosen arbitrarily as indicated above in the derivation of the equations.

The transformation parameter σ varies only very little with the Reynolds number R_x for $F \simeq 2 \times 10^{-3}$ for all injection rates for the compressible flow investigated. The influence of the denominator on $d\sigma/dR_x$ is therefore less significant than for injection rates considerably different from 2×10^{-3}. Since the empirical relationships defining c_f^* and θ^* which are subject to some uncertainties, have only a slight influence on the transformation parameter σ and

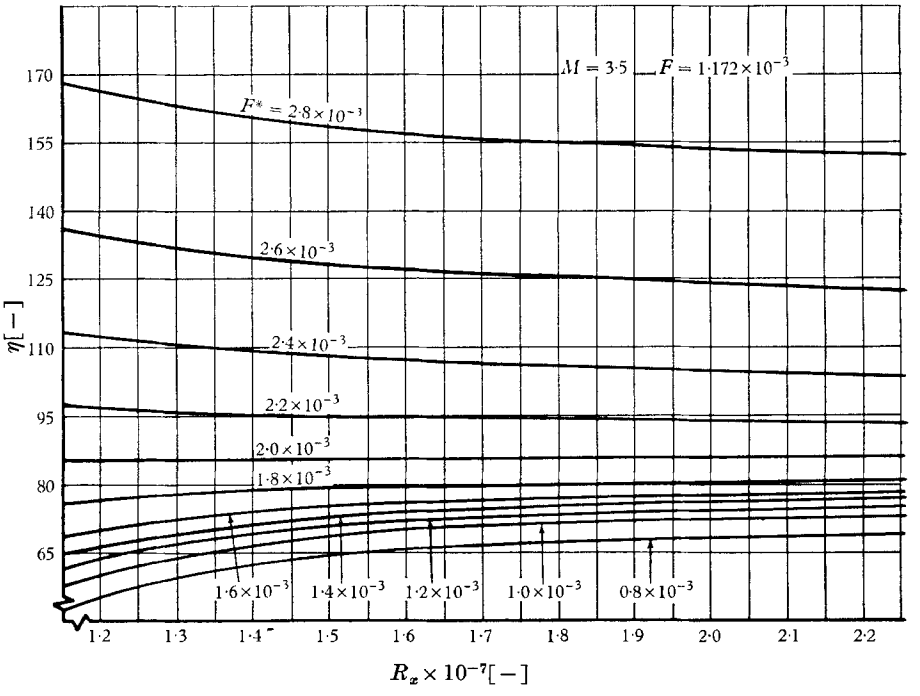

FIGURE 5. Variation of the transformation parameter η with the Reynolds number R_x.

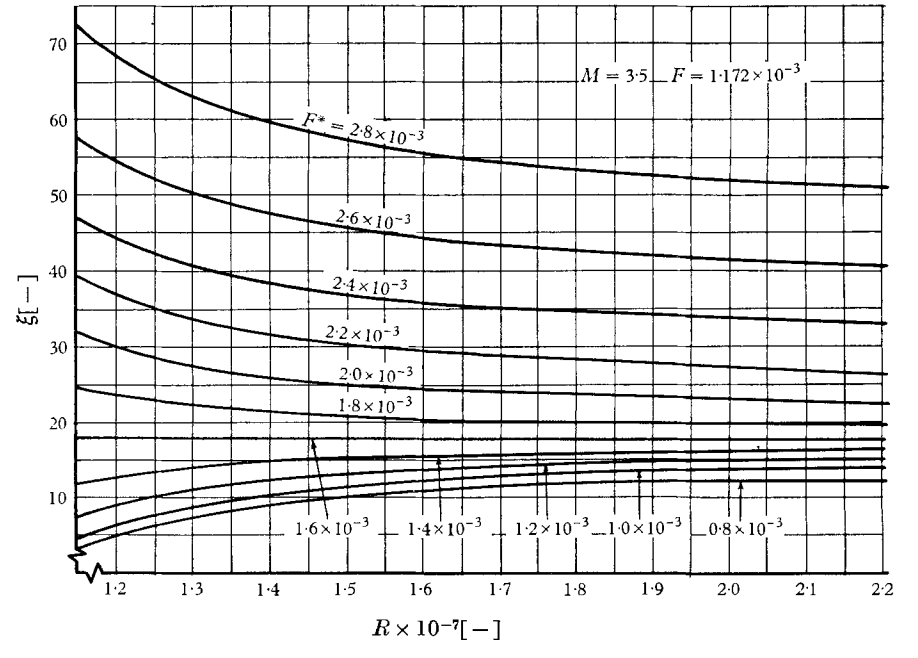

FIGURE 6. Variation of the transformation parameter ξ with Reynolds number R_x.

hence on the transformation itself, an incompressible flow with an injection rate of $F^* = 2 \times 10^{-3}$ has been mainly chosen in § 3 when the transformation will be applied to measured compressible turbulent boundary layers.

2.2.4. *Coles's substructure hypothesis and the present transformation*

Coles needed a third relationship in order to establish his transformation. Thus he introduced the sublayer hypothesis. This sublayer, or substructure, analysis was based on the 'law of the wall' for boundary layers along solid surfaces, namely

$$\frac{u^*}{u_\tau^*} = \frac{1}{\kappa} \ln \frac{y^* u_\tau^*}{\nu^*} + C, \tag{2.29}$$

with the skin friction velocity $u_\tau^* = (\tau_w^*/\rho^*)^{\frac{1}{2}}$, the mixing length theory constant κ and C = constant, assuming that there exists a sublayer Reynolds number defined by a suitable numerical value (indicated by the subscript s) for the product

$$R_s = \frac{u_s^*}{u_\tau^*} \frac{u_\tau^* y_s^*}{\nu_s^*} = \frac{u_s^* y_s^*}{\nu_s^*} = \text{constant} \tag{2.30}$$

(for details see Coles (1962)). The value of R_s was determined from an analysis of experimental data. Furthermore, Coles found that the viscosity had similar properties to the values of σ/μ^* required to correlate measured skin-friction coefficients in compressible flow with the corresponding incompressible values. Thus he assumed that σ/μ^* was in fact equal to μ_s so that

$$\sigma = \mu^*/\mu_s.$$

Further, since $\mu_\infty \leqslant \mu_s \leqslant \mu_w$, σ must lie in the range

$$\mu^*/\mu_w \leqslant \sigma \leqslant \mu^*/\mu_\infty$$

and tend to μ^*/μ_w for increasing Reynolds number.

Hence a potential starting point for a formal extension of Coles's substructure hypothesis to the present problem would be Stevenson's (1963) 'law of the wall' for transpired boundary layers

$$\frac{2u_\tau^*}{v_w^*} \left\{ \left(1 + \frac{v_w^* u^*}{u_\tau^{*2}} \right)^{\frac{1}{2}} - 1 \right\} = \frac{1}{\kappa} \ln \frac{y^* u_\tau^*}{\nu^*} + C \tag{2.31}$$

and determining the product

$$R_s = \frac{2u_\tau^*}{v_w^*} \left\{ \left(1 + \frac{v_w^* u_s^*}{u_\tau^{*2}} \right)^{\frac{1}{2}} - 1 \right\} \frac{y_s^* u_\tau^*}{\nu_s^*} = \text{constant}, \tag{2.32}$$

corresponding to (2.30).

The essential result of this approach is that σ can again be put equal to μ^*/μ_s when one considers several secondary conditions (for details see Jeromin 1966*b*). Hence the transformation parameter σ would lie between the same limits as for the solid wall case: σ would approach μ^*/μ_w for high Reynolds numbers and μ^*/μ_∞ for low Reynolds numbers, say those representing laminar flow, independently of which injection mass flow F^* has been chosen. This result is a contradiction to equation (2.13) which defines σ such that

(i) σ is steadily increasing for R_x = constant and increasing F^* and is not approaching a limiting value for high or low Reynolds numbers as predicted by the substructure hypothesis (see figure 4);

(ii) an injection mass flow can always be chosen arbitrarily so that σ exceeds at least one of the limiting values predicted above.

Moreover, the argument that σ should approach μ^*/μ_∞ for low Reynolds numbers is a contradiction to the present transformation concept when it is extended to laminar flow. Establishing a transformation for laminar flow which is based again on the stream functions and hence on (2.11) would lead to the result that

$$\sigma = A \frac{1}{\rho^* v_w^*} \tag{2.33}$$

and hence not approaching the value μ^*/μ_∞ independently of which injection mass flow has been chosen (for details see Jeromin 1966*a*).

Summarizing, one can say that the substructure hypothesis is breaking down for boundary layers with injection. In particular the values of $\sigma(x)$ eventually found did not lie in the range $\mu^*/\mu_w \leqslant \sigma \leqslant \mu^*/\mu_\infty$; thus it appears that for injection one is not justified in identifying σ/μ^* with μ_s.

3. The application of the transformations

3.1. *Zero injection*

In this section the proposed boundary-layer transformation will be applied to profiles measured by the author (see Jeromin 1966*a*). Measured profiles with zero injection have been analysed by applying to them the transformations of Spence (1960), Mager (1962) and Coles (1962) respectively. As representative formulae for incompressible flow were chosen Ludwieg & Tillmann's (1950) skin friction law and the 'law of the wall' (equation (2.29)) with the constants proposed by Coles (1962) of $\kappa = 0{\cdot}410$ and $C = 5{\cdot}00$. These two formulae give the best agreement with measurements in incompressible turbulent boundary layers.† For this purpose the measured compressible boundary-layer profiles were transformed into corresponding incompressible flows, the skin friction coefficient evaluated from well-established formulae for incompressible flow and the resultant value c_f^* transformed back into compressible flow. Mager's transformation gives skin-friction coefficients which are much lower in the order of 50 % than the experimental values for both the transformed Ludwieg & Tillmann formulae‡ and the 'law of the wall'. In the original paper Mager used another skin friction law $c_{f0}^* = 0{\cdot}0592\,(R_x^*)^{-0{\cdot}2}$ which predicts far higher skin friction coefficients than the formula used here so that the error in his transformation is compensated

† There is a considerable scatter in the literature regarding the actual value of the two constants in the 'law of the wall' (see, for example, Black & Sarnecki 1958). The constants seem to be highly influenced by surface roughness, turbulence level and slight three-dimensional effects—the main parameters which change from investigation to investigation. Coles's constants were chosen because they are good mean values.

‡ Ludwieg & Tillmann's skin friction formula for turbulent boundary layers along solid flat plates is

$$c_{f0}^* = 0{\cdot}246 \times 10^{-0{\cdot}678 H_0^*} R_{\theta 0}^{*\,-0{\cdot}268}$$

(index 0 refers to zero injection).

in his paper by the skin friction law with the result that the agreement is much better. It must, however, be stressed at this point that this skin friction law is obsolete and does not agree with recent measurements in incompressible flow

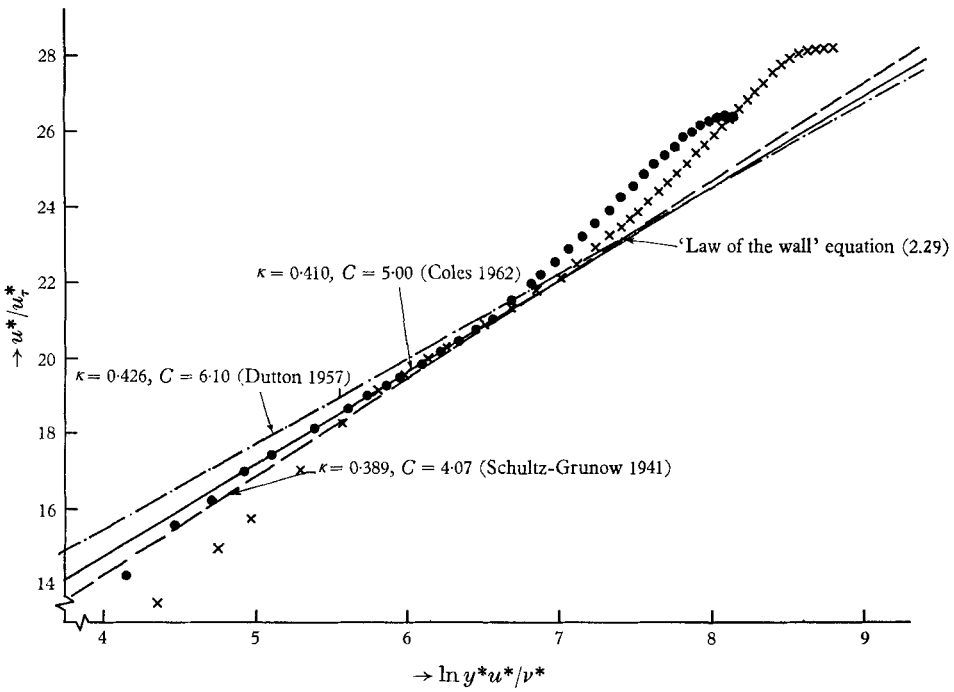

FIGURE 7. Comparison between transformed compressible turbulent boundary-layer profiles measured along solid flat plates, and the ' law of the wall ' for incompressible flow using Coles's transformation ($T_w > T_r$).

Symbol [−]	Run [−]	M [−]	R_θ^* [−]	R_x^* [−]
●	2·5–0·0–1·60	2·5	14,900	$\simeq 2{\cdot}10^7$
×	3·5–0·0–1·60	3·5	7,930	

Assumed corresponding incompressible flow
$u_\infty^* = 16{\cdot}0$ [m/s]
$t^* = 20$ [°C]
$p^* = 1$ [atm]
$F^* = 0$

and hence provides no reasonable check of a transformation. Spence's transformation predicts higher skin-friction coefficients, but the values are of the order of 30 % lower than measured data. Coles's transformation predicts higher skin-friction coefficients than those experimentally determined. It must be emphasized in this connexion that all these measured data are subject to an error of the order of at least 10 % so that both Spence's and Coles's transformation can be considered as reasonable approximations. Two measured compressible boundary-layer profiles (which are representative of all measured profiles for zero injection) are plotted on figure 7 in the transformed stage applying Coles's transformation to the 'law of the wall'. The quantities for the chosen incompressible flow are

specified on the diagrams.† The fully turbulent region could be reduced very well to the 'law of the wall' for incompressible flow. The Reynolds number $R^*_{\theta 0}$ for the transformed compressible boundary-layer profile measured at a Mach number of 2·5 is approximately two times higher than the one measured at a Mach number of 3·5 so that the whole profile for $M = 2{\cdot}5$ is shifted to the right. This shift to the right with increasing Reynolds number $R^*_{\theta 0}$ was also found for incompressible flow. The influence of the Reynolds number is one of the reasons why the outer part of the profile could not be collapsed on one incompressible profile. Moreover, one would expect such a reduction only by plotting the outer region of the profile in appropriate co-ordinates such as

$$\frac{u^*_\infty - u^*}{u^*_\tau} = f\left(\frac{y^*}{(\delta)^*}\right)$$

of the 'velocity defect law', for example. This must remain the subject of a separate investigation and is mentioned here only for reasons of completeness.

In this connexion the attention has to be drawn again to the investigation of Baronti & Libby (1966) which was mentioned in the introduction. They obtained the same excellent collapse for the fully turbulent region of compressible boundary-layer profiles up to a Mach number of 6 when they applied Coles's transformation assuming that the Reynolds number associated with the laminar sublayer is invariant against the transformation instead of using Coles's sublayer hypothesis.

3.2. *Present transformation*

The exact transformation presented in this paper was applied to measured compressible boundary layers with air injection assuming in the case of heat transfer at the wall that this effect is negligible. Only the approximate method has been used to study the effect of heat transfer on the transformation. It was postulated and partly verified for the present transformation that an incompressible flow with an injection rate F^* can be chosen arbitrarily within a certain range. This postulate has been checked on figure 8 for two representative compressible boundary layers measured at a Mach number of 3·5 for two different injection rates (see Jeromin 1966*b*). These two profiles were chosen at random and can be considered as being representative for all the other profiles. The fully turbulent part of the compressible transpired boundary-layer profiles has been reduced to Stevenson's 'law of the wall' for incompressible flow independent of which injection rate F^* was chosen. Only injection rates F^* up to 3×10^{-3} can be checked for the time being, since the transformation parameter cannot be evaluated accurately enough for higher injection rates. This restriction is due to the condition defining the starting point of the integration of (2.13), namely

$$c^*_f F^* R^*_x = 10.$$

For injection rates F^* higher than 3×10^{-3} this condition results in a starting point for the integration of $R^*_{x1} > 4 \times 10^7$ and hence in a Reynolds number range

† The friction velocity u^*_τ was evaluated by transforming the compressible turbulent boundary-layer profile into the corresponding incompressible one and then solving 'the law of the wall' for the transformed profile. In this manner the skin-friction coefficient will be obtained which fits most closely the 'law of the wall'.

which is not covered by the empirical relations defining the skin-friction coefficient and the momentum thickness for incompressible flow. On figure 8 the collapse for the fully turbulent region is excellent for all injection rates F^* chosen. The skin-friction coefficient evaluated for these compressible profiles from Stevenson's 'law of the wall' is independent of the choice of F^*. Again a collapse for the outer part of the compressible profile cannot be expected because of the different Reynolds numbers R_x^* and R_θ^*. This phenomenon will be discussed in more detail later.

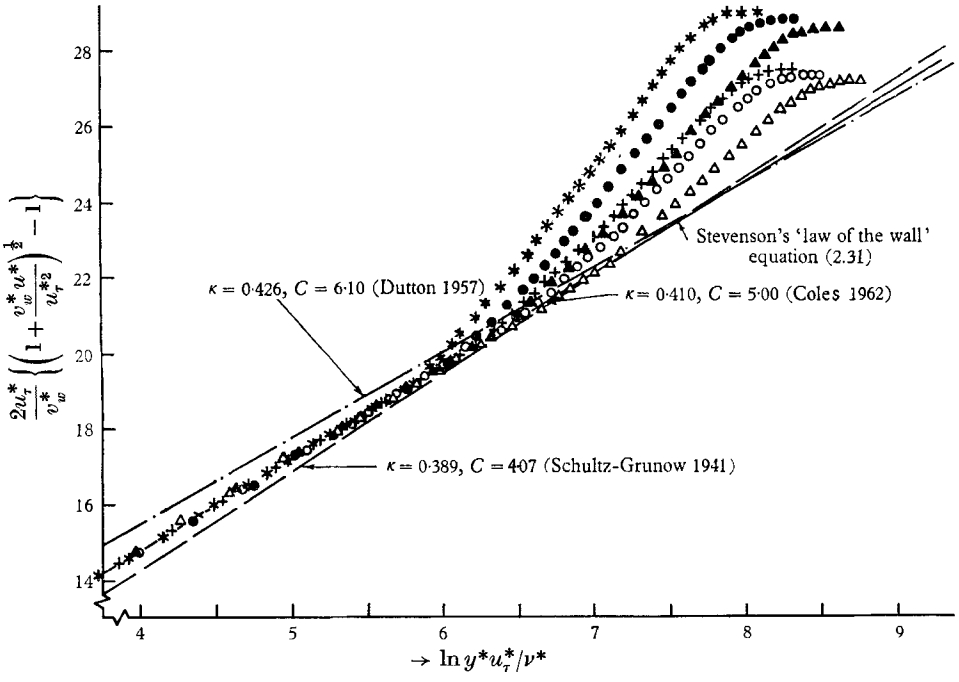

FIGURE 8. Comparison between transformed compressible turbulent boundary-layer profiles with air injection and Stevenson's 'law of the wall' ($T_w > T_r$, three different F^*).

Assumed corresponding incompressible flow

$u_\infty^* = 16{\cdot}0$ [m/s]
$1 \leqslant F^* \times 10^3 \leqslant 2{\cdot}8$
$t^* = 20$ [°C]
$p^* = 1$ [atm]

$M = 3{\cdot}5 \qquad R_x \simeq 2 \times 10^7 \qquad T_w > T_r$

Symbol [−]	Run [−]	$F^* \times 10^3$ [−]	$F \times 10^3$ [−]	$R_x^* \times 10^{-6}$ [−]	R_θ^* [−]
+	3·5–0·6–1·90	1	0·664	6·70	11,900
*	3·5–1·2–1·90	1	1·176	13·05	16,800
○	3·5–0·6–1·90	2	0·664	5·35	19,100
●	3·5–1·2–1·90	2	1·176	7·67	19,700
△	3·5–0·6–1·90	2·8	0·664	6·41	32,000
▲	3·5–1·2–1·90	2·8	1·176	9·89	35,600

Figure 9 is representative of all compressible boundary layers measured at Mach numbers of 2·5 and 3·5 with each of three injection rates F at wall temperatures slightly higher than the recovery temperature. The fully turbulent part of the boundary-layer profile is completely transformed again by the transformation. This collapse is not as good for the highest injection rate at

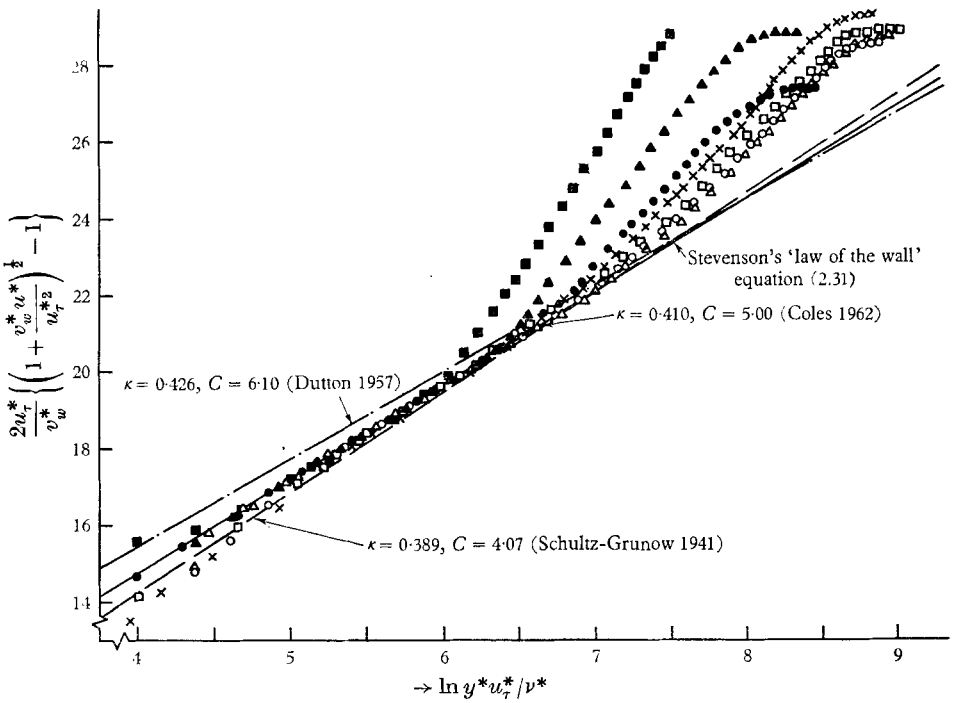

FIGURE 9. Comparison between transformed compressible turbulent boundary-layer profiles with air injection and Stevenson's ' law of the wall' ($T_w > T_r$).

$M = 3{\cdot}5$ $R_x = 2 \times 10^7$ $T_w > T_r$

Symbol [−]	Run [−]	$F \times 10^3$ [−]	$R_x^* \times 10^{-6}$ [−]	R_θ^* [−]
●	3·5–0·6–1·70	0·654	4·47	18,200
▲	3·5–1·2–1·90	1·176	7·71	19,700
■	3·5–2·1–1·90	2·110	12·45	20,150

Assumed corresponding incompressible flow

$u_\infty^* = 16{\cdot}0$ [m/s]
$F^* = 2 \times 10^{-3}$ [−]
$t^* = 20$ [°C]
$p^* = 1$ [atm]

$M = 2{\cdot}5$ $R_x = 2 \times 10^7$ $T_w > T_r$

Symbol [−]	Run [−]	$F \times 10^3$ [−]	$R_x^* \times 10^{-6}$ [−]	R_θ^* [−]
○	2·5–0·5–1·40	0·570	5·47	34,300
△	2·5–0·9–1·60	0·910	8·05	38,300
□	2·5–1·2–1·80	1·270	13·28	35,800
×	2·5–1·3–1·81	1·337	14·56	35,500

$M = 3{\cdot}5$. But this profile is nearly separating (blown-off) so that it is rather surprising that it could be reduced at all. The injection rate for the incompressible flow was chosen to be $F^* = 2 \times 10^{-3}$. The best possible skin-friction coefficient was fitted again to these profiles by solving Stevenson's 'law of the wall' for the transformed compressible flow. The skin-friction coefficient determined from Stevenson's 'law of the wall' is independent of the choice of mass flow parameter F^*.

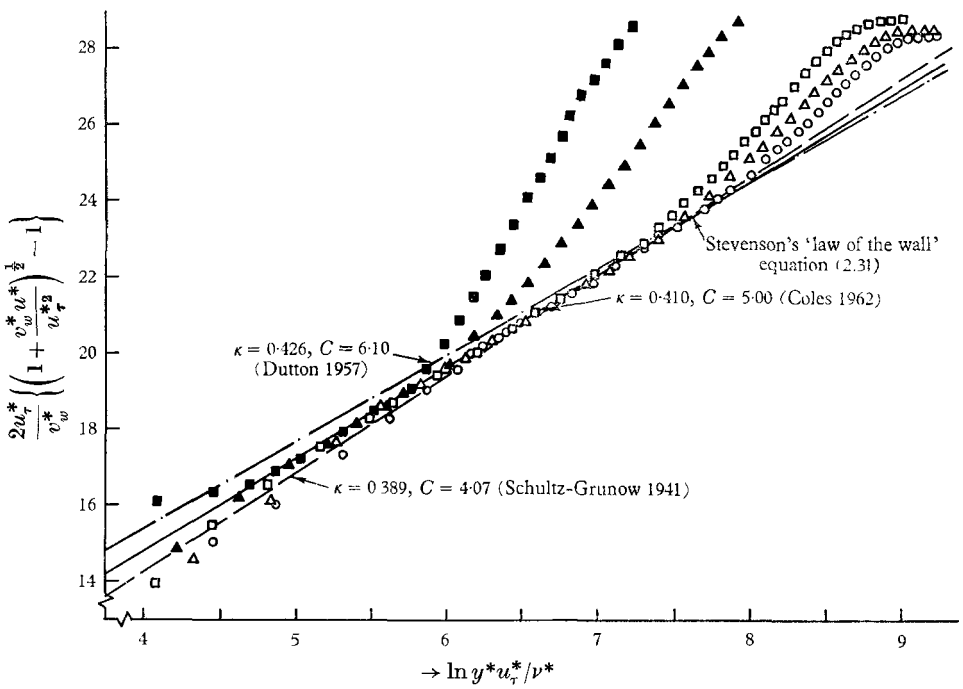

FIGURE 10. Comparison between transformed compressible turbulent boundary-layer profiles with air injection and Stevenson's 'law of the wall' ($T_w \simeq T_r$).

$M = 3{\cdot}5$ $\quad R_x \simeq 2 \times 10^7$ $\quad T_w \simeq T_r$

Symbol [−]	Run [−]	$F \times 10^3$ [−]	$R_x^* \times 10^{-6}$ [−]	R_θ^* [−]
▲	3·5–1·2–2·90	1·204	7·60	17,400
■	3·5–2·2–2·90	2·220	12·05	21,300

Assumed corresponding incompressible flow

$u_\infty^* = 16{\cdot}0$ [m/s]
$F^* = 2 \times 10^{-3}$ [−]
$t^* = 20$ [°C]
$p^* = 1$ [atm]

$M = 2{\cdot}5$ $\quad R_x \simeq 2 \times 10^7$ $\quad T_w \simeq T_r$

Symbol [−]	Run [−]	$F \times 10^3$ [−]	$R_x^* \times 10^{-6}$ [−]	R_θ^* [−]
○	2·5–0·4–2·70	0·416	5·61	36,800
△	2·5–0·8–2·70	0·790	8·15	38,600
□	2·5–1·2–2·70	1·285	13·15	37,300

As one would expect the transformations are best for compressible boundary layers measured at exactly adiabatic wall conditions. Such profiles are plotted in the transformed stage on figure 10 and compared again with Stevenson's 'law of the wall'. The agreement is again excellent for the fully turbulent region. There seems to be a big discrepancy between the profiles measured at a Mach number of 2·5 and those obtained for $M = 3{\cdot}5$, especially for the outer part of the profile. This applies for all the diagrams concerning Stevenson's 'law of the wall'. The reason for this discrepancy is again the different Reynolds number for the transformed compressible flow. This number is about twice as high for the profiles obtained for a Mach number of 2·5 than those for $M = 3{\cdot}5$. McQuaid (1966) showed that the profiles which he measured in incompressible flow shift to the right (the level of $y^*u_\tau^*/\nu^*$ increases) for increasing Reynolds number when the profile is plotted in Stevenson's co-ordinates. At the same time the overall length of the fully turbulent region increases with an increasing R_θ^*. These are exactly the same features as found for the transformed flow as one can see, for example, on figure 10.

3.3. *A general discussion of the results of the transformation*

The skin friction coefficients evaluated for the measured boundary-layer profiles with air injection by applying the transformation (F^* is chosen to 2×10^{-3}) to Stevenson's 'law of the wall' (c_{f2} in the table) and the empirical relation (see appendix) defining c_f^* in (2.13) (c_{f3} in the table) are compared with experimental data in the table below for both Mach numbers investigated.

M	$F \times 10^3$	$c_{f1} \times 10^3$	$\Delta c_{f1} \times 10^3$	$c_{f2} \times 10^3$	$c_{f3} \times 10^3$
2·55	0	1·60	±0·10	1·87	1·62
2·53	0·570	1·15	±0·12	1·08	1·17
2·53	0·895	0·97	±0·15	0·93	0·945
2·54	1·277	0·725	±0·20	0·72	0·73
3·58	0	1·18	±0·10	1·27	1·27
3·56	0·652	0·79	±0·12	0·71	0·77
3·55	1·17	0·56	±0·15	0·47	0·56
3·52	2·11	0·37	±0·20	0·21	0·35

TABLE 1. Comparison of the skin-friction coefficients.

The agreement between the skin-friction coefficient predicted by the transformation and the one calculated directly from the momentum equation (c_{f1} in the table) is excellent at a Mach number of 2·5 for all injection rates investigated. The agreement is not quite as good for $M = 3{\cdot}5$ most probably because of the slight adverse pressure gradient† (for details see Jeromin 1966*b*) which could

† The pressure gradient can be expressed in terms of the momentum equation with

$$\frac{c_f}{2} = \frac{d\theta}{dx} - F - P \quad \text{with} \quad P = \frac{\theta}{\rho_\infty u_\infty^2}\frac{dp}{dx}(2 + H - M_\infty^2).$$

The order of magnitude of the different terms is as follows:

$$\frac{d\theta}{dx} \simeq 1{\cdot}5 \times 10^{-3}, \quad F \simeq 1 \times 10^{-3}, \quad P \simeq -0{\cdot}05 \times 10^{-3}.$$

not be avoided for this Mach number and which is probably overestimated by the 'law of the wall' compared to the momentum equation.

The most realistic values for the skin-friction coefficient of the measured profiles are most probably those evaluated from Stevenson's 'law of the wall' used in connexion with the present boundary-layer transformation. The error for the skin-friction coefficient determined from the momentum equation in creases with increasing injection rate and is included in the table in column 4. The possible error is considerable especially for the highest injection rate at a Mach number of 3·5 where the boundary layer is nearly blown off.

Finally, c_f/c_{f0} is plotted against $2F/c_{f0}$ on figure 11 and compared with all available experimental data. It can be deduced from this figure that the present boundary-layer transformation in connexion with Stevenson's law is the only theoretical approach which predicts the correct order of magnitude of the Mach number influence on the skin-friction coefficient.

It has, moreover, been shown that the transformation also succeeds with respect to the momentum thickness. On figure 12 $R^*_{\theta 0}/R^*_\theta$ is plotted against $F^*R^*_{\theta 0}$. (For details about figure 12 see appendix.) To avoid possible effects of the integration process of (2.18) on the transformation, incompressible flows with injection rates F^* such that $d\sigma/dx$ is approximately zero ($d\sigma/dx \to 0$ for $\sigma \to A$) were chosen. The parameter σ is therefore not influenced by the integration process for which the knowledge of the momentum thickness for the incompressible flow is essential. The transformed values of the momentum thickness are indicated on figure 12 by large symbols, whereas the small ones represent incompressible flow; the drawn lines are $R^*_x = \text{const.}$ For lower Reynolds numbers R^*_x of the order of 5×10^6 the transformed momentum thicknesses lie close to the line which represents the momentum thickness for the highest Reynolds number R^*_x investigated by McQuaid (1966) in incompressible flow of $2{\cdot}5 \times 10^6$. The transformed momentum thickness which lies in a much higher Reynolds number range for R^*_x than covered by incompressible data suggests that the lines $R^*_x = \text{const.}$ still shift in the direction of the arrow with increasing Reynolds number. More measurements in incompressible flow are necessary to confirm this result.

The final conclusion is that the transformation for zero heat transfer succeeds surprisingly well in transforming the compressible turbulent boundary layer with air injection into corresponding incompressible flows even for flows with low heat transfer rates at the wall. The present transformation concept has been formally extended by the author to flows with heat transfer and pressure gradients (for details see Jeromin 1966*a*). Unfortunately these transformations cannot be applied at present because of lack of information about the corresponding incompressible flows so that the possibility of the extension of the present boundary-layer transformation to more complicated flows will be just mentioned here.

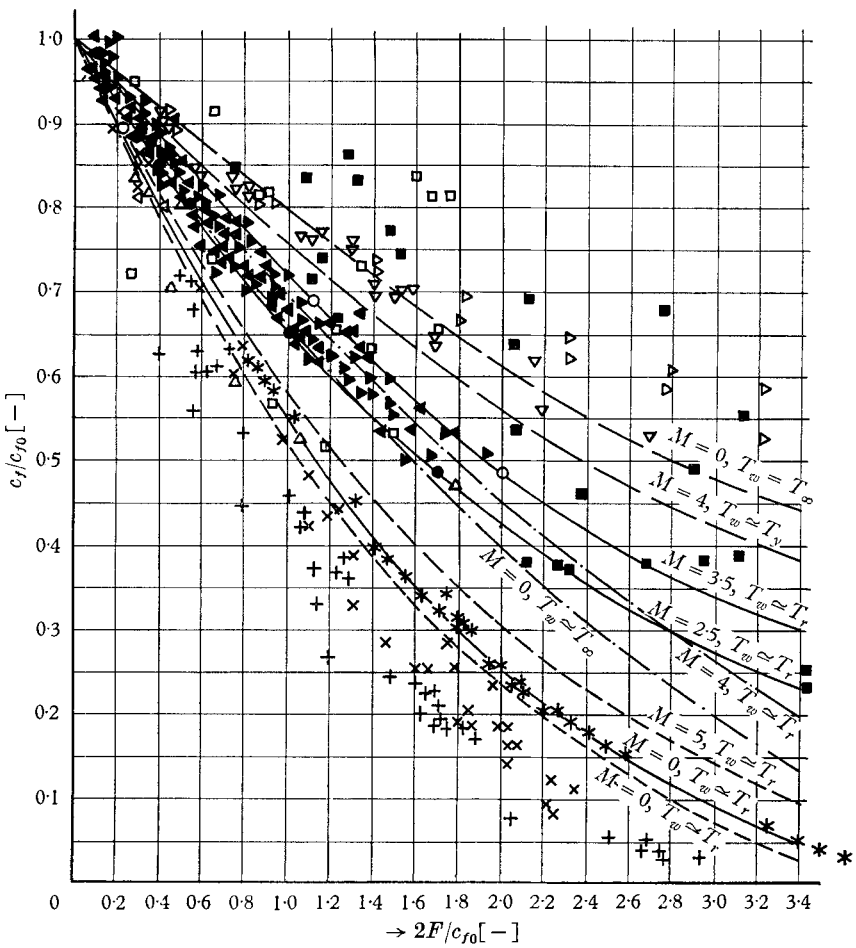

FIGURE 11. Effect of air injection on the skin friction coefficient of a turbulent boundary layer.

Symbol	Investigator	Mach number	Geometry
+	Mickley & Davies (1957)	incompressible	flat plate
×	Romanenko & Kharchenko (1963)	incompressible	flat plate
*	McQuaid (1966)	incompressible	flat plate
▷	Rubesin (1956)	0; 2·0; 2·7	flat plate
□	Danberg (1960)	5·1	flat plate
■	Danberg (1964)	6·1	
●, ○	Jeromin (1966*b*)	2·5, 3·5	flat plate
△, ◁, ▽, ▷	Pappas & Okuno (1960)	0·3, 0·7, 3·5, 4·5	cone
◀	Rubesin (1956)	0; 2·0; 2·7	cone
▶	Tendeland & Okuno (1956)	2·7	cone

For theories see facing page.

Theories

——, present investigation ((equation (2.31) + present transformation);

– – – –, Dorrance & Dore (1954);

—·—, Rubesin (1956);

— —, Spalding, Auslander & Sundaram (1964).

4. Conclusions

(i) The boundary-layer transformations for turbulent boundary layers with air injection have been presented which transform the compressible boundary-layer equations into corresponding incompressible ones.

(ii) The skin-friction coefficient c_f, the momentum thickness θ and the fully turbulent part of the boundary-layer profile in the region where Stevenson's 'law of the wall' applies have been transformed into the corresponding incompressible flow.

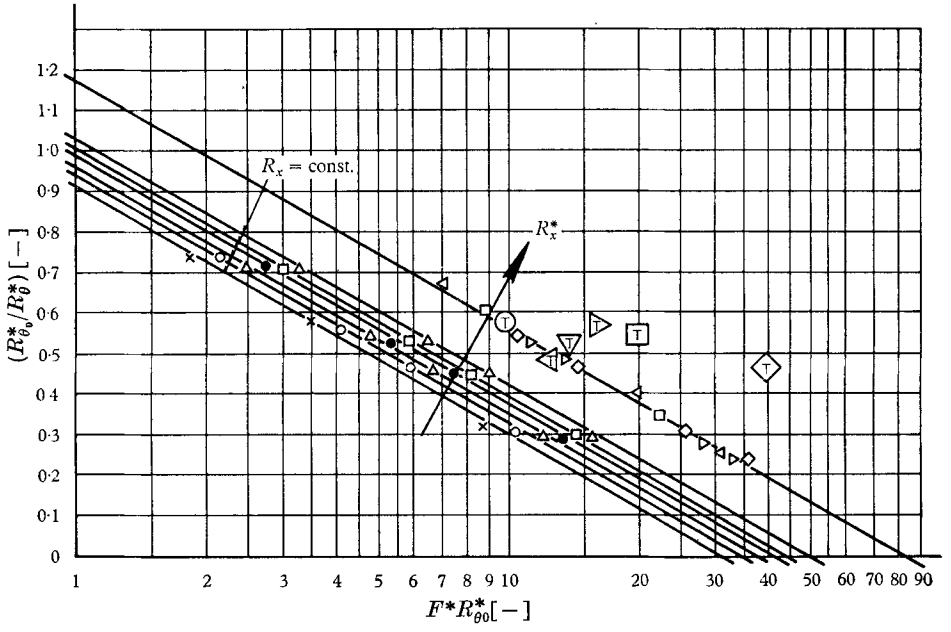

FIGURE 12. The transformation of the Reynolds number R_θ based on the momentum thickness (dimensionless plot with R_{θ_0})

	Transformed compressible flow		
Symbol	Run	$F^* \times 10^3$	$R^*_x \times 10^{-6}$
◁	2·5–0·5–1·10 to 2·5–0·5–1·100	1·2	5·6
▽	2·5–0·9–1·10 to 2·5–0·9–1·100	1·4	8·3
▷	2·5–1·2–1·10 to 2·5–1·2–1·100	1·8	10·4

Incompressible flow
McQuaid (1966)

Symbol	$R_x^* \times 10^{-5}$
×	4·6
○	5·7
△	6·6
●	7·5
□	8·2
▲	9·0
◁	11·1
■	13·2
◇	16·3
▷	19·0
◀	21·5
▶	23·6
◆	26·0

Transformed compressible flow

Symbol	Run	$F^* \times 10^3$	$R_x^* \times 10^{-6}$
Ⓣ	3·5–0·6–1·10 to 3·5–0·6–1·100	1·4	4·6
◘	3·5–1·2–1·10 to 3·5–1·2–1·100	2·0	6·75
◈	3·5–2·1–1·10 to 3·5–2·1–1·90	2·5	11·4

It still has to be checked if such a transformation can be established for the region of the profile where the 'velocity defect law' holds. Another interesting point is to check the validity of the transformation most generally by investigating if the shear stress profiles of the compressible boundary layer can be reduced to corresponding incompressible ones.

(iii) Possibilities for extensions of the transformations to boundary layers with pressure gradients and heat transfer have been briefly mentioned. These transformations cannot be applied for the time being because of lack of information about the corresponding incompressible flows (for details see Jeromin 1966*a*).

This paper was abstracted from a dissertation submitted to the University of Cambridge for the degree of Doctor of Philosophy. The author wishes to express his gratitude to Dr L. C. Squire for his continued interest, assistance and encouragement during the whole course of research. Many useful discussions with him have contributed to this theoretical investigation and especially to this paper. Thanks are also due to Mr N. B. Surrey and Mr A. Barker and their staffs for their help and advice in the design and manufacture of the experimental equipment.

I should like to express my particular thanks to the Provost and Fellows of King's College for their award of an external studentship and for their support throughout the three academic years of the research.

Appendix. Empirical relations representing the incompressible flow

The skin friction coefficient c_f^* and the momentum thickness θ^* of the incompressible flow must be known as a function of x^* or R_x^* before (2.13) can be integrated. Such relations have been determined from McQuaid's experimental data.

The virtual origins of the analysed flows were estimated by the method proposed by Rubesin, Maydew & Varga (1951) so that the boundary-layer characteristics can be expressed in terms of R_x^* (for details see Jeromin 1966*a*). Based on the estimated virtual origin the calculation for c_f^* and θ^* was as follows:

(i) a polynomial $R_{\theta 0}^* = f(R_x^*)$ was fitted to Smith & Walker's (1958) experimental data by plotting $R_{\theta 0}^*$ against R_x^* (index 0 refers to zero injection);

(ii) the boundary-layer parameter H_0^* was determined by fitting a mean curve through all experimental data $H_0^* = f(R_{\theta 0}^*)$ as collated by Thompson (1964);

(iii) once $R_{\theta 0}^*$ and H_0^* were known, the skin-friction coefficient c_{f0}^* was evaluated from Ludwieg & Tillmann's (1950) law;

(iv) the skin-friction coefficient c_f^* was evaluated from c_{f0}^* by putting a mean curve through McQuaid's (1966) experimental data plotting c_f^*/c_{f0}^* against $2F^*/c_{f0}^*$;

(v) the Reynolds number $R_{\theta 0}^*$ and hence the momentum thickness θ^* was determined by fitting again a polynomial through McQuaid's experimental data by plotting $R_{\theta 0}^*/R_\theta^*$ against $FR_{\theta 0}^*$ (see figure 12). Parameter in such a diagram is the Reynolds number R_x^* which is represented in figure 12 by the lines $R_x^* =$ constant. The small symbols in figure 12 are McQuaid's data. With increasing Reynolds number the lines $R_x^* =$ constant shift in the direction of the arrow as indicated on figure 12.

REFERENCES

Baronti, P. O. & Libby, P. A. 1966 Velocity profiles in turbulent compressible boundary layers. *AIAA J.* **4**, 193–202.

Black, T. J. & Sarnecki, A. J. 1958 The turbulent boundary layer with suction or injection. *British ARC R. & M.* no. 3387.

Coles, D. 1962 The turbulent boundary layer in a compressible fluid. The *RAND Corp. Santa Monica Calif.* R-403-Pr. Also *Phys. Fluids*, **7**, 1403.

Crocco, L. 1963 Transformations of the compressible turbulent boundary layer with heat exchange. *AIAA J.* **1**, 2723–2731.

Czarnecki, K. R. & Sinclair, A. R. 1955 An investigation of the effects of heat transfer on boundary layer transition on a parabolic body of revolution (NACA RM 10) at a Mach number of 1·61. *NACA Rept.* no. 1240.

Danberg, J. F. 1960 Measurements of the characteristics of the compressible turbulent boundary layer with air injection. *NAVORD Rept.* no. 6683. *Aerodyn. Res. Rept.* no. 67.

Danberg, J. F. 1964 Characteristics of the turbulent boundary layer with heat and mass transfer at $M = 6{\cdot}7$, *NOL TR*, 46–99. *Aerodynamic Res. Rept.* no. 228.

Dorrance, W. H. & Dore, F. J. 1954 The effect of mass transfer on the compressible turbulent boundary layer skin friction and heat transfer. *J. Aero/Space Sci.* **21**, 404–410.

Dutton, R. A. 1957 The velocity distribution of a turbulent boundary layer along a flat plate. *ARC C.P.* no. 453.

Dutton, R. A. 1958 The effect of distributed suction on the development of turbulent boundary layers. *ARC* no. 20,036.

Eber, G. R. 1952 Recent investigations of temperature recovery and heat transfer on cones and cylinders in axial flow at the NOL Aeroballistic Wind Tunnel. *J. Aero/Space Sci.* **19**, 303.

HIGGINS, R. N. & PAPPAS, C. C. 1951 An experimental investigation of the effect of surface heating on boundary layer transition on a flat plate in supersonic flow. *NACA TN* no. 2351.

JEROMIN, L. O. F. 1966*a* The compressible turbulent boundary layer with fluid injection. Ph.D. Thesis, University of Cambridge.

JEROMIN, L. O. F. 1966*b* An experimental investigation of the compressible turbulent boundary layer with air injection. *ARC* no. 28,549, *ARC R. & M.* 3526.

LUDWIEG, H. & TILLMANN, W. 1950 Investigations of the wall shearing stress in turbulent boundary layers. *NACA TM* no. 1285.

MAGER, A. 1962 Transformation of the compressible turbulent boundary layer. *J. Aero/Space Sci.* **25**, 305–311.

MCQUAID, J. 1966 Incompressible turbulent boundary layers with distributed injection. Ph.D. Thesis, University of Cambridge.

MICKLEY, H. S. & DAVIES, R. S. 1957 Momentum transfer for flow over a flat plate with blowing. *NACA TN* no. 4017.

PAPPAS, C. C. & OKUNO, A. F. 1960 Measurements of skin friction of the compressible turbulent boundary layer on a cone with foreign gas injection. *J. Aero/Space Sci.* **27**, 321.

ROMANENKO, P. N. & KHARCHENKO, V. N. 1963 The effect of transverse mass flow on heat transfer and friction drag in a turbulent flow of compressible gas along an arbitrarily shaped surface. *Int. J. Heat Mass Transfer*, **6**, 727–738.

ROSENBAUM, H. 1966 Turbulent compressible boundary layer on a flat plate with heat transfer and mass diffusion. *AIAA J.* **4**, 1548–1556.

RUBESIN, M. W. 1956 The influence of surface injection on heat transfer and skin friction associated with the high speed turbulent boundary layer. *NACA R. & M.* A 55 L13.

RUBESIN, M. W. 1959 An analytical estimation of the effect of transpiration cooling on heat transfer and skin friction characteristics of a compressible, turbulent boundary layer. *NACA TN* no. 3341.

RUBESIN, M. W., MAYDEW, R. C. & VARGA, S. A. 1951 An analytical and experimental investigation of the skin friction of the turbulent boundary layer on a flat plate at supersonic speeds. *NACA TN* no. 2305.

SCHERRER, R. 1951 Comparison of theoretical and experimental heat transfer characteristics of bodies of revolution at supersonic speeds. *NACA, Rept.* 1055.

SCHLICHTING, H. 1960 *Boundary Layer Theory*, 4th edition. New York: McGraw-Hill Book Company.

SCHULTZ-GRUNOW, F. 1941 Neues Widerstandsgeretz für glatte Platten. *Luftfahrtforschung* **17**, 239, 1940; *NACA TM* no. 986, 1941.

SMITH, D. W. & WALKER, J. H. 1958 Skin friction measurements in incompresible flow. *NACA TN* no. 4231.

SPALDING, D. B., AUSLANDER, D. M. & SUNDARAM, T. R. 1964 The calculation of heat and mass transfer through the turbulent boundary layer on a flat plate at high Mach numbers, with and without chemical reaction. *Supersonic Flow, Chemical Processes and Radioactive Transfer*, pp. 211–276. Edited D. B. Olfe and V. Zakkay. Oxford: Pergamon Press.

SPENCE, D. A. 1960 Distributions of velocity, enthalpy and shear stress in the compressible turbulent boundary layer on a flat plate. *J. Fluid Mech.* **8**, 368–387.

STEVENSON, T. N. 1963 A law of the wall for turbulent boundary layers with suction or injection. The College of Aeronautics, Cranfield. *CoA Rept. Aero* no. 166.

TENDELAND, T. & OKUNO, A. F. 1956 The effect of fluid injection on the compressible turbulent boundary layer—the effect on skin friction of air injected into the boundary layer of a cone at $M = 2{\cdot}7$. *NACA RM* A 65 D05.

THOMPSON, B. C. J. 1964 A critical review of existing methods of calculating the turbulent boundary layer. *ARC* no. 26109, *ARC F.M.* no. 3492.

VAN DRIEST, E. R. & BOISON, J. C. 1955 Boundary layer stabilization by surface cooling in supersonic flow. *J. Aero/Space Sci.* **22**, 70.